Actively controlled release of Dexamethasone from neural microelectrodes in a chronic *in vivo* study

CrossMark

C. Boehler [a, b, *], C. Kleber [a, b], N. Martini [c], Y. Xie [c], I. Dryg [c], T. Stieglitz [a, b],
U.G. Hofmann [a, c], M. Asplund [a, b]

[a] BrainLinks-BrainTools Center, University of Freiburg, Germany
[b] Department of Microsystems Engineering (IMTEK), University of Freiburg, Germany
[c] Section for Neuroelectronic Systems, Clinic for Neurosurgery, Medical Center — University Freiburg, Germany

ARTICLE INFO

ABSTRACT

Stable interconnection to neurons *in vivo* over long time-periods is critical for the success of future advanced neuroelectronic applications. The inevitable foreign body reaction towards implanted materials challenges the stability and an active intervention strategy would be desirable to treat inflammation locally. Here, we investigate whether controlled release of the anti-inflammatory drug Dexamethasone from flexible neural microelectrodes in the rat hippocampus has an impact on probe-tissue integration over 12 weeks of implantation. The drug was stored in a conducting polymer coating (PEDOT/Dex), selectively deposited on the electrode sites of neural probes, and released on weekly basis by applying a cyclic voltammetry signal in three electrode configuration in fully awake animals. Dex-functionalized probes provided stable recordings and impedance characteristics over the entire chronic study. Histological evaluation after 12 weeks of implantation revealed an overall low degree of inflammation around all flexible probes whereas electrodes exposed to active drug release protocols did have neurons closer to the electrode sites compared to controls. The combination of flexible probe technology with anti-inflammatory coatings accordingly offers a promising approach for enabling long-term stable neural interfaces.

1. Introduction

The development of implantable microelectrodes has revolutionized the field of biomedical applications by enabling bi-directional communication with neural tissue at high resolution. In particular penetrating probes, extending deep into neural structures, allowed substantial progress in the understanding of neuronal pathways and networks [1—4]. They further promoted therapeutic and diagnostic applications like deep brain stimulation (DBS) for treating symptoms of Parkinson's disease or severe psychiatric disorders [5,6]. In addition, brain machine interfaces (BMIs) and associated neuro-prosthetic devices rely on signals recorded from or delivered across such neural electrodes [7—9].

In chronic recordings of electrophysiological signals with penetrating probes it has however been observed that signals attenuate or disappear after only few weeks post implantation [10,11]. This effect is attributed to a foreign body reaction taking place around any object inserted into tissue. In consequence to the insertion trauma along with the disruption of the blood brain barrier as well as the presence of the probe itself, a complex cascade of immune reactions is triggered [12]. These processes can be summarized into two phases relevant for neural probes [11]: An increased concentration of activated microglial cells around the probe, identified by the ED-1 antibody, is characteristic for the acute inflammation phase immediately following the implantation [13]. With progressing time, this acute inflammation develops into a chronic state which is defined by a dense astrocytic scar tissue (identified by glial fibrillary acidic protein (GFAP)) encapsulating the probe [11,14,15]. Along with the accumulation of scar tissue over several weeks, a reduction in the number of neurons in close proximity to the implanted probe has further been observed within a radius of ca. 100 μm around the probe [14,16]. It is to date still unknown whether this loss is caused by the migration of neurons away from the implanted probe, whether neurons are repelled

during the formation of the scar tissue or whether they eventually degenerate by other means in this process. This chronic inflammation state and the loss of close-by neurons impairs the long-term functionality of microelectrodes and ultimately leads to reduction of recorded signal quality. Under these conditions, electrical stimulation parameters need to be continuously adjusted to retain efficient tissue activation over time [10,11,17,18]. For silicon based implants, chronic inflammatory reactions have been found in tissue extending as far as 300 μm [19] or 10 mm [20] away from the probe surface beyond 16 weeks of implantation in the rat or macaque cortex, respectively. In contrast, stab-wounds did not show any persistent inflammation, demonstrating that the probe itself rather than the implantation trauma leads to the chronic inflammation state [19]. Variations in probe geometries and implantation techniques were further not found to result in improved chronic tissue response [21–23].

In order to attenuate the immune reactions towards implanted probes, flexible substrates were introduced aiming at minimizing the mechanical mismatch between the tissue and the probe [24,25]. With this approach, micro-motion associated inflammation was addressed which occurs in consequence to microscopic movements of stiff implants inside soft tissue [11]. Flexible substrate materials, such as polyimide (PI) with a Young's Modulus of ~9 GPa, were reported to provide lower tissue reactions when compared to scar formation described in the literature for stiff silicon implants (Young's modulus of ~180 GPa) [26–28]. Precise insertion of such flexible probes into the cortex however is demanding and requires complex insertion techniques, posing limitations to this approach [29–31]. Attaching biomolecules to the surface of stiff silicon implants has further been shown to reduce neuronal loss in the close vicinity to the probe [32].

Aiming at modifying the biological side rather than the probe itself, delivery of anti-inflammatory drugs has been described as strategy for attenuating chronic immune reactions and was in particular suggested to slow down neurodegeneration [19]. This technology can be used independent of the probe geometry or type and offers the possibility to directly influence the cellular reactions in the close vicinity to the implanted probe. Dexamethasone (Dex) is the most prominent corticosteroid drug described for inflammation attenuation. Several studies demonstrated reduced inflammation when Dex was released from passively eluting substrates (e.g. PLGA microspheres) implanted subcutaneously [33–36] or in the central nervous system [37–42] for times between 6 h and 28 days. The pharmacological efficacy of the drug was not influenced by the storage and subsequent release [36,38]. It has nevertheless been observed that the chronic immune response could not be affected by such passive eluting systems for implantation times beyond 30 days [39,43–45]. This observation demonstrates that pharmacological modulation of the tissue response during the acute inflammation phase is not sufficient but rather sustained delivery technologies with active control over release are required to address the chronic immune reaction.

Conducting polymers (CPs) like poly(3,4-ethylenedioxythiophene) (PEDOT) have been described as promising material for such active release technology in biomedical applications. Introduced as electrode coatings with low impedance and high charge injection capacity for neural probes [46–49], CPs further provide the possibility to incorporate, and thus store, ionic substances such as drugs in their bulk. Controlled release of stored drugs can subsequently be achieved by applying an electrical signal to the CP which enables high temporal control over drug expulsion [50–52]. Proof of concept for actively triggered release of Dex from such systems has been demonstrated *in vitro* from large substrates (0.1–4 cm^2) and for comparably short time frames (minutes to hours) [53–59]. Active drug release *in vitro* over longer time frames

(up to four weeks) has been reported by us in a previous study [60] suggesting that chronic immune response modulation with such release technology is generally feasible. Chronic *in vivo* studies employing micro-scale probes with active drug delivery functionality tested over several months have however not been reported in literature so far. It is therefore still unknown whether such CP release systems provide an efficient means for attenuating the chronic immune response to implanted neural probes at time frames and in dimensions more relevant for clinical applications.

We here target this question by combining the beneficial properties of a flexible neural probe with the active drug delivery properties of CPs. The impact of this probe technology on the chronic immune response is evaluated over 12 weeks *in vivo* employing weekly triggered active release of Dex from PEDOT/Dex coated electrode sites in the rat brain. Electrophysiological, electrochemical and immunohistochemical data are collected from functionalized probes and non-functionalized controls implanted bilaterally in the hippocampus of 12 rats. Thereby techniques promoting stable long-term adhesion for CP coatings as well as strategies for enabling precise insertion of polyimide flex-probes are employed.

2. Materials and methods

2.1. Basic electrode fabrication

Neural probes for *in vitro* and *in vivo* measurements were based on flexible polyimide substrates with a platinum metallization embedded between two polyimide layers, fabricated according to the process described by Stieglitz et al. [24]. In brief, a 5 μm thin polyimide layer was deposited on a carrier wafer. For adhesion promotion, 50 nm of Silicon Carbide (SiC) were deposited on the polyimide in a chemical vapour deposition process [61]. Subsequently, 100 nm of platinum and 400 nm IrOx were sputtered on the polymer substrate and photo-lithographically patterned to define the electrode sites. IrOx thereby served as adhesion promoter for the subsequent PEDOT coatings [62]. Finally, a second polyimide layer of 5 μm thickness was deposited as insulation layer and selectively opened via reactive ion etching to create the electrode sites as well as the contact pads. The resulting flex-probes were 10 μm thin with a shaft of 380 μm width and 15 mm in length. The probes featured 16 individual electrode contacts with 12 electrode sites of 15 × 15 μm^2 and four electrode sites of 50 × 50 μm^2 according to the layout in Fig. 1a. A large ring-aperture, reinforced with a circular platinum electrode, was integrated at the tip of each electrode (Fig. 1a) to serve as guidance for an insertion tool during implantation. The distal end of the probe was designed to fit into a conventional ZIF-connector.

2.2. Deposition of PEDOT/Dex coatings

Aiming at attenuating the foreign body response, the four large electrodes in the midline of the probe shaft were selected for carrying an anti-inflammatory coating. For being able to actively modulate the drug expulsion, this coating was based on the conducting polymer PEDOT. The corticosteroid Dexamethasone 21-phosphate disodium salt (Dex) was incorporated into the PEDOT during the polymerization process and was thus stored in a confined area on the probe. The coating was realized by galvanostatic electropolymerization using an Autolab potentiostat (PGSTAT128N, Metrohm, Filderstadt, Germany) in a three electrode configuration with a stainless steel counter electrode (2 cm^2) and an Ag/AgCl reference electrode. An aqueous solution of 0.01 M EDOT and 0.01 M Dex was used as electrolyte and the deposition was carried out at a current density of 800 μA/cm^2 with a target
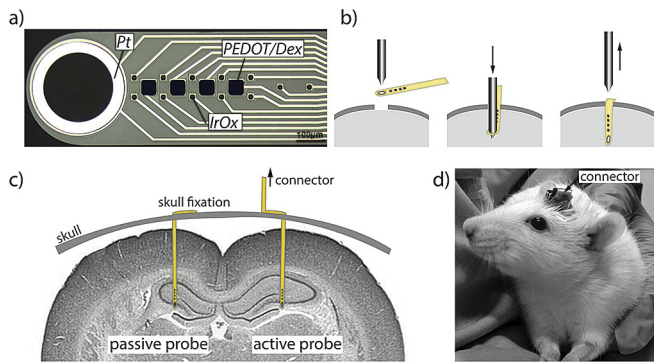
Fig. 1. a) Microscope image of a polyimide neural probe with 4 PEDOT/Dex coated electrode sites shown in blue. Probe insertion is performed according to the process shown in b) with an optical fibre as guiding tool. The final placement of the electrodes can be seen in c). Both the passive probe (control) and the active probe (functionalized) are fixated to the skull. The connection of the active probe to the recording/stimulation equipment is achieved via a connector placed on the head of the animal (d). (For interpretation of the references to colour in this figure legend, the reader is referred to the web version of this article.)

charge density of 300 mC/cm^2. Prior to the polymer deposition, all contact sites were subjected to an electrochemical preconditioning step using cyclic voltammetry (CV) scans (-0.6 V-0.9 V at 0.1 V/s) in phosphate buffered saline (PBS, 0.01 M) until a stable redox-behaviour was observed (typically after 25 scans). Subsequent to the polymerization, all probes were rinsed with Milli-Q water and stored in sterile PBS overnight allowing elution of loosely adsorbed EDOT and Dex on the probe surface before the shafts were implanted.

Besides the anti-inflammatory PEDOT/Dex coatings, also non-functionalized CP coatings were realized on selected probes to serve as controls. The cleaning and deposition parameters were identical to the previously described process, however, sodium polystyrenesulphonate (NaPSS, 5 mg/ml) was used as counter ion instead of Dex. The resulting coatings are hence denoted as PEDOT/PSS. In total 30 probes were prepared, whereas 24 were implanted according to Table 1 and the remaining 6 were subjected to *in vitro* measurements.

2.3. Implantation procedure of Dex-coated probes

All animal experiments conducted in this study were performed with approval from the locally responsible Animal Welfare Committee with the Regierungspräsidium Freiburg in accordance with the guidelines of the European Union Directive 2010/63/UE (permit G13/51). The animal model chosen consisted of twelve adult female Sprague Dawley rats (Charles River, Germany), weighing 280–320 g (avg. 314 g) and maximal efforts were made to minimize the number of animals used with respect to statistical constraints. Prior to surgery, all rats underwent several weeks of handling in order to familiarize them with the experimenter and subsequently enable drug release in fully awake and freely moving animals. The animals were initially sedated with Isoflurane and subsequently anesthetized with Ketamine (100 mg/kg) and Xylazine (3 mg/kg). Disinfectant (Softasept) was applied to the scalp and the surgical field was prepared by shaving the area using small animal shears. Protective ointment (Bepanthen™ eye and nose ointment) was applied to the eyes to prevent drying and to provide a physical barrier during surgery. Anesthetized and shaved rats were placed in a stereotactic frame (Kopf Instruments, Tujunga, USA) with atraumatic ear bars (tooth bar = 0.0). After mid-line incision, the skull was exposed and a total of 8 holes with 0.9 mm diameter were carefully drilled into the skull whereas 6 holes were located in a circular pattern laterally on the skull. Stainless steel screws were inserted into the 6 lateral holes so that the screw heads extended a few mm over the bone. These screws were later used as anchor points for additional stabilization of the dental cement which was used to fix the connector to the skull. The two holes for the actual electrodes were drilled at 3.6 mm posterior and 2.5 mm lateral with respect to bregma. The dura was removed manually using a bent syringe-needle (27G). Each animal received two probes targeting the CA1 region of the hippocampus (DV: -2.2 mm from dura mater). The probe in the left hemisphere always served as material-reference and the probe in the right hemisphere was used for the actual recording/stimulation experiments. A list of the 12 animals with the corresponding probes can be found in Table 1. Insertion of the probes was facilitated with a glass fibre (125 µm diameter without cladding) that was threaded through the ring structure on the tip of the probes and thereby enabled straight insertion of the flexible substrate as indicated in Fig. 1b. This process was modified from the procedure described by Richter et al. and Loeffler et al. [31,63]. After implantation, control probes were fixed to the skull by super glue (cyanoacrylate) and the connection site of the probes was trimmed (see Fig. 1c). Active probes were fixed to the skull in an equal manner, but the connection sites of these probes were inserted into a custom made printed circuit board (PCB) which was then sealed with UV-curable adhesive. The PCB was fixated on the skull using 2 component dental cement (Palapress, Heraeus Holding GmbH, Germany) so that one end of the PCB, carrying an 18-pin Omnetics connector (A79040-001, Omnetics Connector Corporation, USA), remained accessible for connecting the animal to the external recording or stimulation equipment (Fig. 1d). The skin was sutured around the dental cement and the animals were allowed to recover for one week under prophylactic daily administration of Caprofen (Carprieve, Norbrook, UK, 4 mg kg^{-1} s.c.) pain reliever. Animal weights were further regularly measured as indicator for their overall health status during the 12 weeks experimental time. Continuous gain in weight could be observed for all animals, demonstrating good health conditions so that no animal had to be excluded from the experiments.

2.4. Neural recordings

During the first week after surgery, animals were allowed to recover and no drug elution or recordings were performed during this time. In the subsequent weeks, awake and freely moving

Table 1
List of all 12 animals with the implanted probes in the right (R) or left (L) hemisphere.

		1	2	3	4	5	6	7	8	9	10	11	12
PEDOT/Dex	active (CV-stimulation)	R	R	R	R								
PEDOT/Dex	passive (no stimulation)					R	R	R	R				
PEDOT/PSS	active (CV- stimulation)									R	R	R	R
PEDOT/PSS	passive (no stimulation)	L	L	L	L	L	L						
IrOx	passive (no stimulation)							L	L	L	L	L	L

animals were subjected to weekly experimental sessions. Recordings were performed with an RZ5 multichannel recording system (Tucker-Davis Technologies, Alachua, USA) and neural activity was simultaneously recorded from all 16 electrode sites on the probe over 120 s at a sampling rate of 40 kHz. Local Field Potentials (LFPs) were extracted from these data by low pass-filtering (300 Hz) directly during data acquisition. Further data filtering was performed offline after analog-digital conversion using the program NeuroExplorer4 (Nex Technologies, Madison, USA) where a low pass filter (40 Hz cutoff frequency, 10th order lowpass) was used to eliminate the 50 Hz noise.

2.5. Impedance spectroscopy measurements

Following neural recordings, the animals were connected to a potentiostat (PGSTAT 204, Metrohm, Filderstadt, Germany) for *in vivo* impedance measurements. Here only the four PEDOT-coated electrode sites were used on each probe and individually connected as working electrode in a three electrode configuration. The platinum ring structure on the probe-tip was used as counter electrode and a small IrOx electrode located in the centre of the probe served as reference electrode (Fig. 1a), forming an electrochemical cell directly on the probe. Suitability of IrOx as (pseudo) reference material in biomedical applications has previously been described by Shinwari et al. [64] and Yang et al. [65]. Care was taken to ensure a firm connection and the open circuit potential (OCP) was observed for at least 10 s to confirm stable electrode configuration. The impedance spectrum was then recorded between 1 Hz and 10 kHz using sinusoidal excitation signals with an amplitude of 10 mV. This measurement was done for all animals, regardless of the polymer coating type.

Impedance measurements from *in vitro* probes were performed in the same electrode configuration with identical settings in 0.01 M PBS.

2.6. On-demand drug release in vivo

Controlled release of Dex for attenuation of the foreign body response to the implant was performed on a weekly basis (starting at week 2 post op *in vivo*). Drug elution was triggered subsequently to the impedance measurements in the fully awake and mobile animal using the same electrode configuration. A CV-signal was successively applied to each of the four coated electrode spots per probe and drug release was triggered by three CV scans between -0.6 V and 0.15 V (vs. the IrOx reference) at a scan speed of 0.1 V/s. The potentiostat was programmed with both voltage and current limitations (-0.65 V, 0.2 V and 10 μA) in order to keep the stimulation sub-threshold for neuronal effects and to avoid unpredictable current flow. This ensured animal safety at any time during the drug release process. Over the 12 weeks, these limits were never reached or exceeded. In addition, no behavioural response was ever observed during the 45 s of CV-stimulation, confirming sub-threshold stimulation.

Identical CV-sweeps were applied to the group of animals implanted with active PEDOT/PSS probes. In this case no release of the PSS can be expected as consequence to the immobilized bulky PSS anion. These animals serve as control group to evaluate the effect of the stimulation signal on the immune response intensity in contrast to the release of Dex from the PEDOT/Dex probes. CV curves were further used to determine the CSC by integrating the area under the curves. The CSC thereby serves in parallel as measure for the electrode status, which has previously also been described by Alba et al. *in vivo* [66] and by Boehler et al. [62] for long-term monitoring of electrode properties *in vitro*.

2.7. Histology and image analysis

Following 12 weeks of implantation, all animals were put in deep anaesthesia using 300 mg/kg Ketamine and 9 mg/kg Xylazine i.p. and subsequently *trans*-cardially perfused by paraformaldehyde and PBS. All flex-probes, except for one which was explanted for SEM imaging, remained in the tissue and care was taken while removing the connector and extracting the brain to keep the electrodes in position. Removed brains were stored in fixation solution (4% paraformaldehyde) for one week at 4 °C before they were transferred into sucrose solution (30% in PBS). For immunohistochemical staining of neurons and inflammation markers (reactive microglia and astrocytes), 20 μm thin tissue slices were prepared with a cryostat-microtome (CM 3050 S, Leica, Wetzlar, Germany) and transferred to glass slides. Brain slices were then divided into two groups according to their consecutive numbering (even/odd) so that a co-staining with the cell specific markers NeuN, GFAP and DAPI (for visualization of neurons, reactive astrocytes and cell nuclei) could be performed on slices with even numbers and respectively a co-staining with ED1, GFAP and DAPI (for visualization of reactive microglia, reactive astrocytes and cell nuclei) on slices with odd numbers. Using this technique, only three fluorescence channels were required for imaging of the slices and high spatial resolution could be retained by altering ED1 and NeuN staining in steps of only 20 μm. Prior to antibody incubation, all slices were exposed to 10% normal donkey serum (NDS) for 30 min to block unspecific binding. Subsequently, both groups were exposed to NeuN (mouse IgG), GFAP (polyclonal rabbit antibody) and ED1 (mouse IgG) for 3 h. Alexa Fluor488 donkey anti mouse (λ_{ex}: 495 nm, λ_{em}: 519 nm) and Alexa Fluor647 donkey anti rabbit (λ_{ex}: 649 nm, λ_{em}: 666 nm) were used as secondary antibody and incubated for 1 h each. Staining of cell nuclei was ensured by the use of Dapi-Fluoromount G (λ_{ex}: 358 nm, λ_{em}: 461 nm) for fixing the slices on the glass slides. Fluorescence imaging of these slices was performed within 24 h after staining with a Nikon Eclipse Ti-S inverted microscope (Nikon, Duesseldorf, Germany) equipped with a CCD colour camera. Image analysis was subsequently done with ImageJ where GFAP and ED1 fluorescence intensity profiles in front of the electrode were determined as measure for the immune response to the electrode. The auto-fluorescence of the polyimide probe (observed in all fluorescence channels at 461, 519 and 666 nm) enabled a precise reconstruction of the electrode sites along the probe shaft and consequently highly accurate measurements. Fluorescence intensity and thus distribution of relevant cells was assessed in each slice along a 50 μm wide region of interest (ROI) extending 300 μm away from the electrode surface as indicated in Fig. 8b. Data obtained from all tissue slices containing a fragment of the PEDOT-coated electrode sites were subsequently averaged to yield an intensity-distance profile for the different animal groups. Neuron distance was measured between NeuN stained cell bodies and PEDOT/Dex coated electrode sites along a straight line representing the shortest distance between the two objects.

2.8. In vitro measurements

Six PEDOT/Dex functionalized probes, fabricated equally to the animal probes, were stored in 37 °C PBS during the time course of the animal study. During these 12 weeks, three of the *in vitro* probes were regularly CV-cycled in analogy to the implanted peers. All *in vitro* probes received weekly impedance measurements. Data from these probes were used to evaluate progressive impedance and charge storage capacity (CSC) changes of the PEDOT coatings in absence of the *in vivo* environment and these probes were further used as controls for SEM imaging.

Drug release parameters employed in this study were generally based on previous work from Boehler et al. where active release of Dex from PEDOT/Dex probes has been investigated in response to CV cycling *in vitro* over multiple release events and over several weeks [60]. Selection of an appropriate CV-range and implementation of adhesion promotion were thereby described as critical parameters for enabling Dex release and restricting EDOT leakage. Based on this data, and with the intention to avoid undesired electrochemical reactions *in vivo*, we choose a CV-range of −0.3−0.45 V vs. Ag/AgCl for drug release in our animal study. In order to account for the reduced CV range, compared to the previously reported data (−0.6−0.9 V vs. Ag/AgCl), the Dex-release properties were re-evaluated *in vitro* prior to the actual animal experiment in this work. A test electrode (4 mm diameter, in analogy to previous work) was coated with PEDOT/Dex and repeatedly exposed to CV-based release cycles over a total time of 45 days. Active and passive drug expulsion in PBS were analysed by high performance liquid chromatography (HPLC) in this time frame following the previously described protocols [60]. Drug release was further evaluated for PEDOT/Dex coatings deposited on either platinum or IrOx substrates to evaluate the influence of the substrate material on the release characteristics. For this test, polyimide based probes were fabricated in analogy to the final implants to ensure relevant test conditions. Release characteristics of these samples were assessed over three active release events within 150 min.

2.9. High magnification imaging of the probes

At the endpoint of the study, one of the probes carrying four electrode sites with a PEDOT/Dex coating was explanted instead of sliced. The probe was carefully rinsed with Milli-Q water and transferred to PBS where CV and EIS measurements were performed. The explant was further imaged by Scanning Electron Microscopy (SEM) using a Nova NanoSEM (FEI, Hillsboro, USA) to evaluate the status of the coating after 12 weeks *in vivo*. The morphology of these PEDOT sites was subsequently compared to SEM images of PEDOT/Dex films exposed to CV cycling over 12 weeks *in vitro* as well as pristine PEDOT/Dex films imaged directly after electrodeposition of the coating.

2.10. Statistical analysis

Statistical significance of data was analysed by OriginPro (OriginLab Corporation, version 2016G) and XLSTAT (Addinsoft, version 19.01) software. Anderson-Darling tests were used to confirm normal distribution of values before either Student t-tests or Wilcoxon signed-rank-test were performed. P-values <0.01 were considered significant.

3. Results

3.1. In vitro drug release

The drug release profile of PEDOT/Dex electrodes was investigated *in vitro* over a time period of 45 days with active release events on day 10, 14, 42 and 45 employing 5 CV scans (−0.3−0.45 V vs. Ag/AgCl) per release event for evaluation of release efficiency. Quantification of released Dex by HPLC analysis thereby revealed a total amount of 805 ng of Dex being released within 45 days. 24% of this mass were attributed to actively triggered release within 0.006% of the total experiment time, demonstrating a substantial release in response to the CV sweeps compared to purely passive drug elution. The largest drug expulsion was found during the first trigger event (114 ng) while subsequent release events featured an

average drug expulsion of 25 ± 12 ng. Drug was thereby released within a time of 1 min per active release event. For the passive drug elution an average mass of 0.006 ± 0.005 ng could be measured in the respective timeframe. Evaluation of drug release from PEDOT/Dex films deposited on either platinum or IrOx substrates revealed in both cases an active contribution of 19% to the totally eluted mass in 2% of the total time. This demonstrates that drug release characteristics are not influenced by the substrate material.

3.2. Neural recordings

Electrophysiological data were collected on a weekly basis from the implanted neural probes and used to evaluate the recording capability of the PEDOT-coated electrode sites during the chronic study. LFP signals from all 12 animals at week 12 post implantation are summarized in Fig. 2a demonstrating unrestricted neural recording functionality until the end of the study for all implanted probes. The detailed spectral analysis of these LFP-data showed a strong signal contribution in the low LFP band between 2 Hz and 15 Hz (Fig. 2b). This spectral composition was found consistent over the 12 weeks as can be seen from the representative data at week 6 and 12 in Fig. 2b.

3.3. Electrochemical measurements in vivo

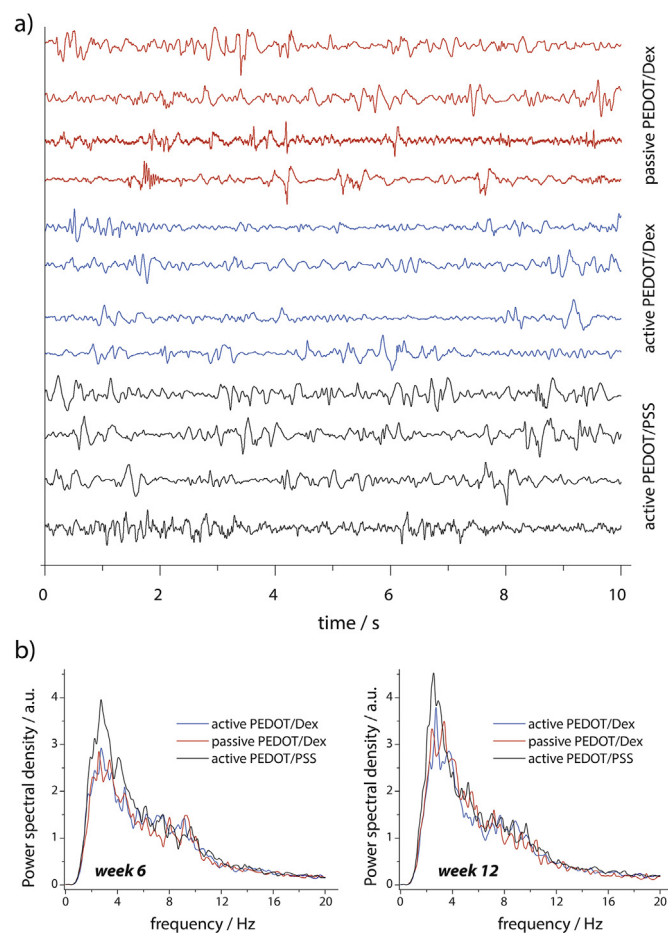The signal employed for drug release was simultaneously used

Fig. 2. a) Representative LFP data recorded after 12 weeks *in vivo* from 12 animals demonstrating persistent recording capability for PEDOT/Dex and PEDOT/PSS coated probes. Spectral analysis shows presence of low frequency LFPs over the entire study time (b).

to calculate the CSC by integrating the total area under the CV-curves which provides a measure for the electrode status. CSC-values for active PEDOT/Dex animals and active PEDOT/PSS
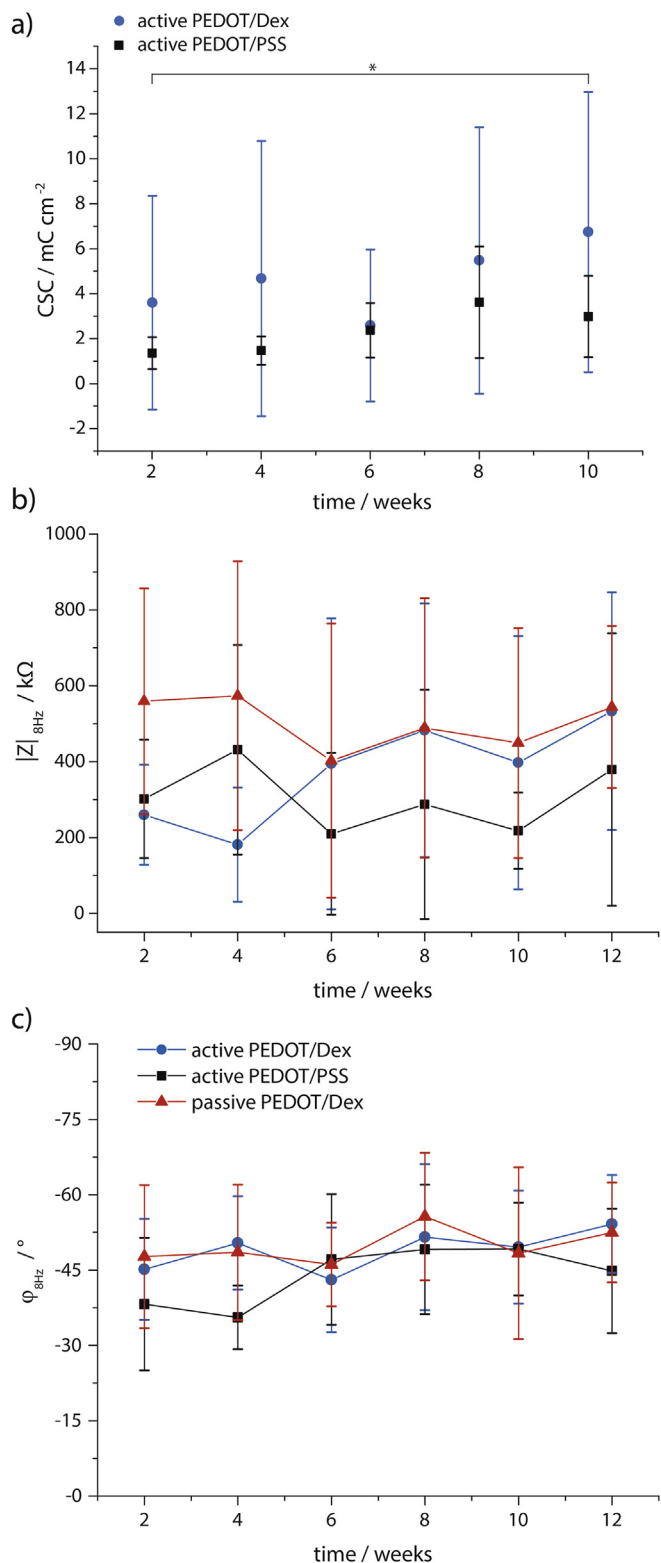

Fig. 3. Electrochemical data recorded over 12 weeks *in vivo* for monitoring of the PEDOT properties. CSC (a), Impedance magnitude (b) and phase angle (c) display averaged data for the different animal groups with standard deviation as error bars (n = 16). The horizontal line indicates statistical difference for active PEDOT/PSS (p < 0.01).

animals are summarized in Fig. 3a where each data point represents the average over 4 probes from 4 animals (n = 16). For both animal groups, an increase in the CSC can be seen with progressive time while the absolute CSC for the PEDOT/Dex probes was found overall higher compared to the PEDOT/PSS controls by an average factor of 2.1. The observed difference between the two groups was however not statistically significant (p > 0.01) over the 12 weeks. Between week 2 and week 10 post implantation a CSC increase of 91% (from 3.6 to 6.8 mC cm^{-2}) and 120% (from 1.4 to 3.0 mC cm^{-2}) for the PEDOT/Dex probes and the PEDOT/PSS probes could be measured respectively. The increase for PEDOT/PSS controls was thereby statistically significant (p < 0.01) whereas the increase for PEDOT/Dex probes was not statistically significant (p > 0.01).

Electrochemical impedance spectroscopy (EIS) data, recorded over 12 weeks and averaged within the three animal groups, was further used to verify the status of the polymer electrodes while being implanted. Results from these measurements are displayed in Fig. 3b for the impedance magnitude and Fig. 3c for the corresponding phase angle. Based on the main signal contribution in the low LFP spectrum (between 2 and 15 Hz), a frequency of 8 Hz has been chosen for comparing the different polymer coatings. The active PEDOT/Dex probes showed initially the lowest impedance until week four post implantation when an increase could be seen from 260 kΩ at week two to 533 kΩ at week 12. The impedance for the passive PEDOT/Dex probes was found consistently higher from the beginning with 559 kΩ at week two and 544 kΩ at week 12. While the PEDOT/PSS probes featured an initial impedance of 302 kΩ at week two, these probes were measured with the lowest impedance at the end of the study (379 kΩ at week 12). Besides these impedance alterations within the different animal groups it is however worth mentioning that overall a maximum impedance change of a factor two could be seen during the entire study which is here considered as stable impedance behaviour. Variability in impedance data within the three test groups (data averaged over 4 animals) could also be seen within individual animals. Furthermore, no statistically significant differences (p > 0.01) in the impedance data were observed between the different groups. The same impedance behaviour could be observed at a frequency of 1 kHz for the different coatings (data not shown), demonstrating that impedance was stable regardless of frequency. The phase angle showed a slight decrease over the 12 weeks from −45° to −54° (+20%) for the active PEDOT/Dex probes, −39° to −45° (+15%) for the active PEDOT/PSS probes and −48° to −52° (+8%) for the passive PEDOT/Dex implants (Fig. 3c). The observed decrease was thereby not statistically significant.

The full impedance spectrum recorded from 1 Hz to 10 kHz is displayed in Fig. 4 for all material groups at week 12 post implantation (n = 16). All coating types feature similar impedance characteristics over the full frequency spectrum as seen in the impedance magnitude (Fig. 4a) and for the phase angle (Fig. 4b). Impedance values close to a frequency of 50 Hz were influenced by noise from the 50 Hz power supply and therefore show the highest variations in the measurement. Average phase angles over the complete frequency spectrum were −54° (±14°), −53° (±14°) and −53° (±12°) for active PEDOT/PSS, active PEDOT/Dex and passive PEDOT/Dex groups respectively (n = 160).

3.4. Electrochemical measurements in vitro

In parallel to the *in vivo* experiments, six PEDOT/Dex coated probes were exposed to 37 °C PBS over 12 weeks for monitoring the electrode properties *in vitro* and providing reference data to the implanted probes. CV and impedance measurements were performed in analogy to the implanted peers on weekly basis. The CSC data from three actuated probes is shown in Fig. 5a where a
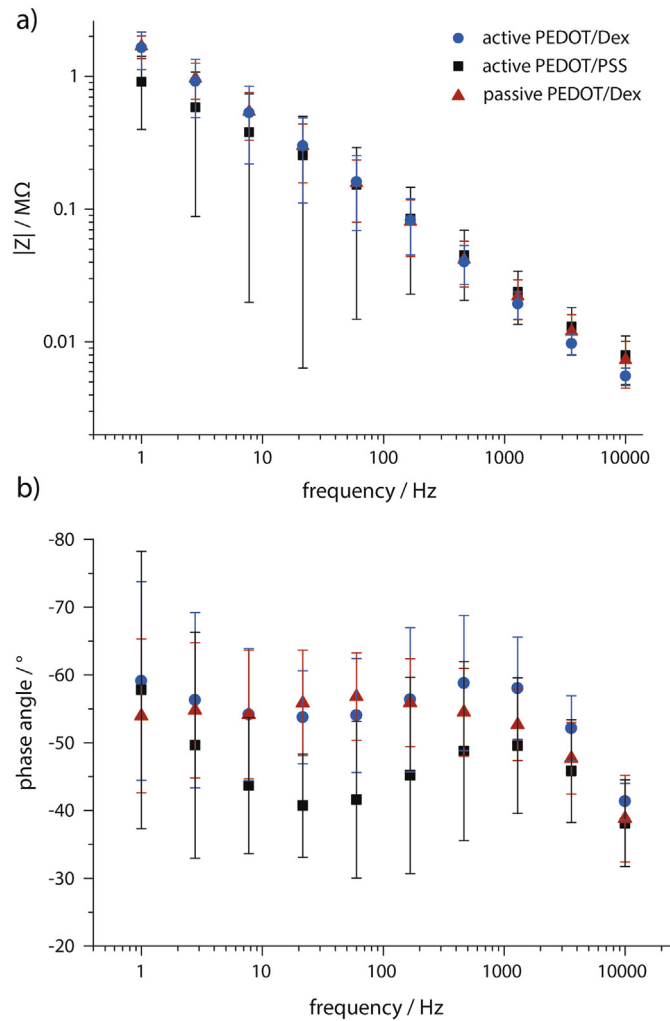
Fig. 4. EIS spectrum recorded at week 12 post implantation shows similar characteristics for all animal groups in the impedance magnitude (a) and for the phase angle (b). Error bars denote standard deviation (n = 16).

statistically significant (p < 0.01) increase in the CSC from 0.58 to 0.73 mC cm^{-2} can be seen with progressing storage time. The CSC-increment of 26% between week two and week 10 was substantially lower compared to the *in vivo* probes (91% increase). Furthermore, the values measured *in vitro* were found overall lower compared to the CSC measured *in vivo* (e.g. 0.73 ± 0.09 mCcm^{-2} vs. 6.7 ± 4.2 mCcm^{-2} at week 10 post implantation).

Fig. 5b displays the impedance magnitude at 8 Hz, averaged over all *in vitro*-probes. During the storage time of 12 weeks, a statistically significant increase (p < 0.01) in the impedance can be seen, approaching a value of 270 kΩ towards the end of the measurement time. This value represents half of what has been measured for the active PEDOT/Dex probes during the *in vivo* measurements (533 kΩ). The phase angle in the *in vitro* EIS measurements (displayed in Fig. 5c) shows a progressive decrease during the experiment time from −71° at week two to −79° at week 12. The difference of 11% is thereby similar to the changes observed from the *in vivo* data (20%). An offset of −20° between the phase angles determined *in vivo* and *in vitro* could be measured, attributed to the different complexity of the electrolytes. Optical microscopy revealed that all PEDOT coatings were fully intact and adherent to the *in vitro* probes after 12 weeks in PBS storage.
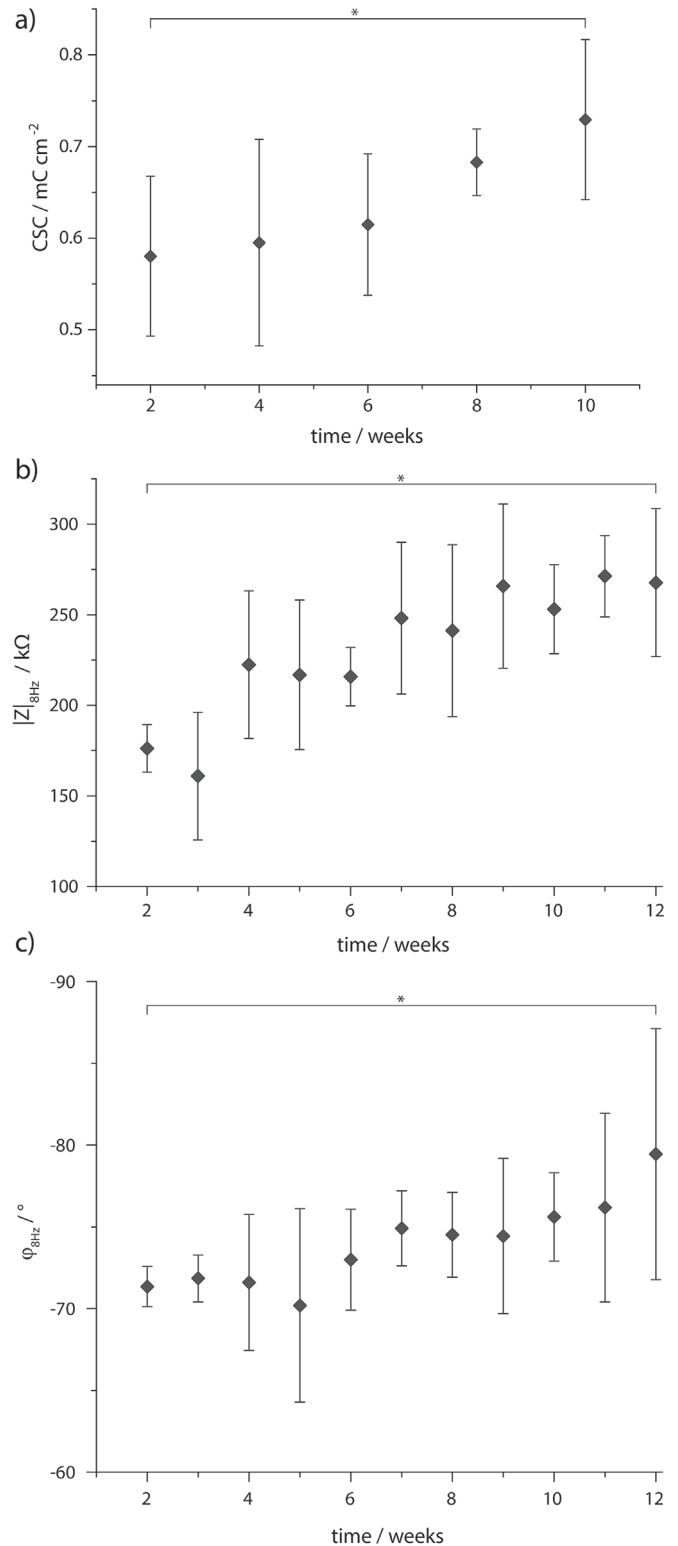

Fig. 5. Electrochemical data measured *in vitro* from three PEDOT/Dex probes. Averaged data for CSC (a), impedance magnitude (b) and phase angle (c) originate from n = 12 electrode sites, error bars denote standard deviation. The horizontal line indicates statistical difference (p < 0.01).

3.5. Examination of the explanted probe

At the endpoint of the study, one PEDOT/Dex probe was

explanted and used for electrochemical measurements as well as SEM imaging to verify the status of the coating. In Fig. 6a the CSC for the explanted probe is compared to the corresponding values before the probe was implanted and to an uncoated IrOx surface. After deposition of the PEDOT/Dex, the CSC was measured with 2.78 mCcm^{-2} which represents an increase of 28% compared to the uncoated IrOx (2.18 mCcm^{-2}). Following explantation and rinsing of the probe with PBS, a CSC of 7.15 mCcm^{-2} could be measured which is 2.57 times higher compared to the status before implantation. From the impedance data in Fig. 6b it can further be seen that the impedance of the electrode sites was lower when measured after explantation (153 kΩ at 8 Hz) compared to the status before implantation (239 kΩ at 8 Hz). The impedance of the uncoated IrOx was overall highest with 304 kΩ at a frequency of 8 Hz. Comparing the low impedance after 12 weeks *in vivo* with the initial values of IrOx demonstrates that the polymer coating was still intact at the endpoint of the study. This observation could be confirmed by SEM imaging of the probe where a homogenous coverage of the electrode sites with PEDOT/Dex could be seen (Fig. 6c). Higher magnification of the electrode sites revealed a highly roughened surface of the polymer coating for the explant (Fig. 6f) which is comparable to the morphology of a PEDOT/Dex sample stimulated over 12 weeks *in vitro* (Fig. 6e). Both probes thereby revealed a larger grain size in comparison to a pristine PEDOT/Dex sample (Fig. 6d) indicating a morphological change for the exposed coatings during the 12 weeks which explains the observed changes in CSC and EIS.

3.6. Immunohistochemical analysis

In order to evaluate the intensity of the foreign body reaction towards the implanted probes after 12 weeks *in vivo*, the retrieved tissue was horizontally sliced, with the probe remaining in the tissue, and immunohistochemically stained. Staining was thereby done for GFAP, NeuN and ED1 which provides information about the chronic formation of scar tissue, neuron survival and microglia activity in the probe vicinity respectively. By keeping the probe in the tissue during slicing, and making use of the auto-fluorescence of the polyimide substrate, it was possible to precisely identify the exact location of the PEDOT-coated electrode sites from the histology pictures (Fig. 7). Quantitative image analysis could therefore be performed with direct correlation to the coated sites along the probe shaft. Fig. 8a displays the measured distance between the electrode sites and the nearest neurons identified from NeuN stained images. With a distance of only 10 μm, the closest neurons were found in front of the active PEDOT/Dex probes as well as the passive IrOx implants. For the remaining PEDOT coatings, a minimal distance of 16–30 μm could be measured. The average neuron to electrode distance for all investigated materials was between 48 and 83 μm with the lowest distance observed for the active PEDOT/Dex probes. Differences in mean neuron distance between the different sample groups were however not statistically significant (p > 0.01).

GFAP fluorescence intensity was used to evaluate the thickness of the astrocytic scar tissue which formed around the electrode within the 12 weeks study. Fluorescence intensity profiles along a 300 μm long ROI extending from the probe surface (see inset in Fig. 8b) were averaged over all slices per animal group. An overall decrease in the intensity within a distance of 75 μm from the electrode site could be seen for all samples (Fig. 8b). GFAP fluorescence, and thus astrocyte scar formation, was found lowest at the electrode surface for the IrOx probes while all PEDOT coated probes showed similar astrocyte counts in close distance to the probe surface, regardless of the counter ion. The observed difference between the IrOx control and passive PSS probes was not
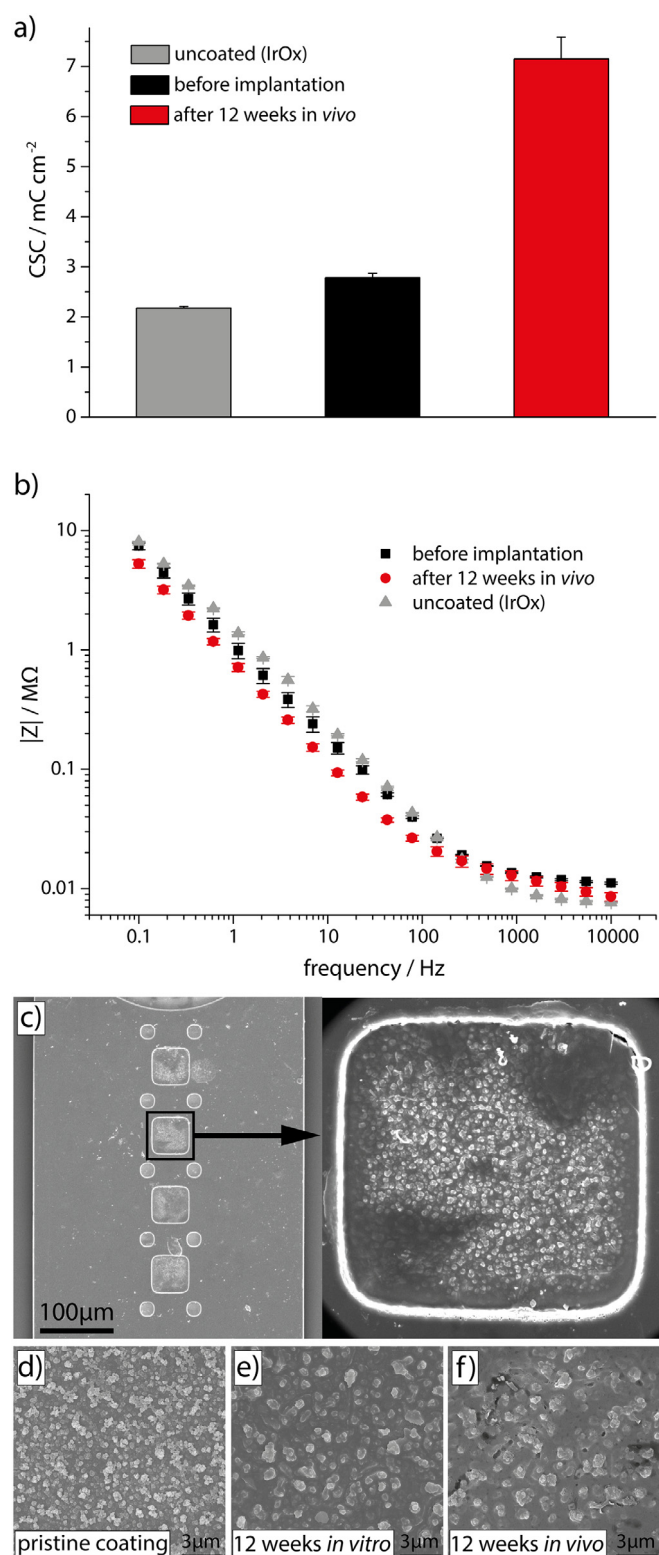

Fig. 6. Comparison of CSC (a) and impedance magnitude (b) for a PEDOT/Dex coated probe before implantation and after 12 weeks *in vivo*. Error bars denote standard deviation (n = 4). High resolution SEM shows fully intact PEDOT/Dex coatings after 12 weeks of implantation (c) during which 30 CVs have been applied for drug release. Dark areas in the higher magnification image result from tissue residues after explantation. The morphology of explanted PEDOT/Dex coatings (f) is comparable to PEDOT/Dex films exposed to *in vitro* stimulation over 12 weeks (e) and shows larger grains in comparison to a pristine polymer film directly imaged after polymerization (d).
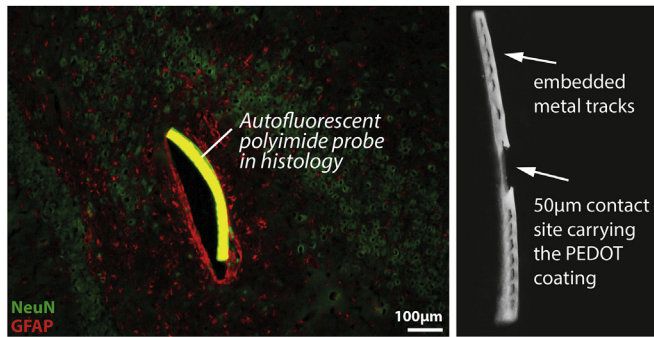
Fig. 7. Auto-fluorescent polyimide probes permit simple probe identification in histology and enable precise correlation of tissue reactions with functionalized areas on the probe.
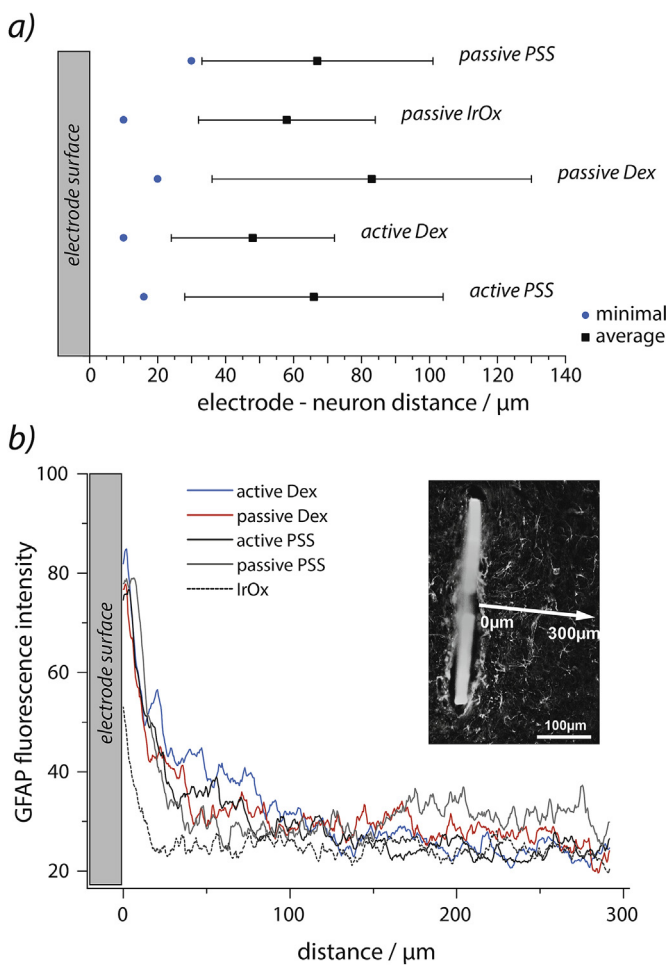

Fig. 8. Neuron distance (a) and GFAP fluorescence intensity (b) for different coating materials on the polyimide probes. The inset in (b) shows the path along which the GFAP fluorescence intensity was measured and averaged using a 50 μm wide ROI. Data represents average over n = 30, error bars in a) denote standard deviation.

statistically significant at any distance. GFAP intensity differences were significant (p < 0.01) within 30 μm (active PSS), 35 μm (passive PSS) and 70 μm (active Dex) between IrOx and the respective polymer coated probes. At distances exceeding 75 μm from the electrode surface, no difference in GFAP staining between the tested materials could be seen resulting in a baseline level of astrocyte density at 75—300 μm distance. This baseline level could

further be confirmed by GFAP measurements from reference tissue slices at different implantation depths and locations, corresponding to inflammation-free tissue. Differences in GFAP intensity among the polymer coated probes were not statistically significant (p > 0.01).

ED1-staining, representing activated macrophages/microglia, showed a lower intensity in close vicinity to the PEDOT/Dex probes as compared to PEDOT/PSS probes as can be seen from the fluorescence intensity profiles in Fig. 9. This difference was however not found to be statistically significant (p > 0.01). Active or passive probes within these two material classes thereby only showed minor differences in ED1 intensity. The overall lowest microglia intensity could be found directly in front of the IrOx implants, the difference to the polymer coated probes was however not statistically significant. At distances exceeding 20 μm from the electrode surface, no difference between the probes types could be observed in ED1 fluorescence.

4. Discussion

Neural microprobes provide excellent opportunities for biomedical research and clinical applications by providing highly selective recording or stimulation of neural tissue. Following implantation, these probes however inevitably trigger a foreign body response leading to chronic scar tissue formation which ultimately affects usability in long-term applications.

This study combines two of the most promising technologies for making long-term stable connection to neuronal tissue possible over chronic periods of time: flexible probes and anti-inflammatory treatment in the form of local drug delivery. Dex release from flexible thin-film probes, implanted in the rat hippocampus, was studied over a period of 12 weeks which is to our knowledge the first time that active driven drug release has been investigated *in vivo* over such a long period of time.

Dex has previously been tested as anti-inflammatory treatment either administered locally by passive eluting systems [33,35—42,45] or in the form of systemic treatment [34,67]. In the latter case, practical applicability has however been limited considering the high systemic dose needed in order to reach efficient levels locally at the surface of an implant. Dex is a corticosteroid drug and has well
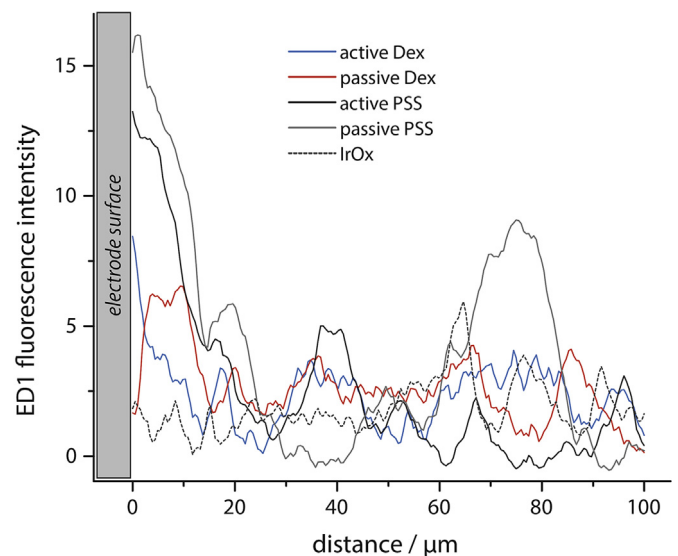

Fig. 9. ED1-staining for microglia activity shows lower intensity for PEDOT/Dex probes compared to PEDOT/PSS controls.

documented and serious side effects at high concentrations. A PEDOT release system circumvents the systemic side effects by enabling highly local administration of the drug directly at the electrode site. Furthermore, and in contrast to coatings based on biodegradation or diffusion for delivery, it offers superior temporal control over release. Dosage of a drug can thereby be scheduled to specific time points over a relatively long time frame, or even be provided in response to a surveillance parameter, e.g. related to inflammation status.

We here test the hypothesis that anti-inflammatory treatment, extending beyond the initial healing phase of six weeks, could have an impact on probe-tissue integration also on the longer perspective. Our study covers 12 weeks which extends well into what is generally considered to be representative for chronic conditions. Data collected over this time frame indicate that electrodes exposed to an active Dex delivery protocol on a weekly basis did have neurons closer to the electrode sites than any of the control materials in the study. Such a neuron-protective effect of Dex has previously been assumed from *in vitro* studies [53] and could be supported from our chronic measurements *in vivo*. Given the relatively small number of animals and probes included in the study, and the small differences seen, it is however not possible to draw any statistically significant conclusion ($p > 0.01$) on the positive impact of Dex on overall probe performance. In fact, the use of flexible polyimide probes already reduced the extent of inflammation to a level where the criteria for stable recordings are already fulfilled regardless of the electrode coating material. Nevertheless, several important conclusions can be drawn pointing the way for future work with anti-inflammatory electrodes.

Over a period of 12 weeks we performed in total 320 stimulation sessions with either PEDOT/Dex or PEDOT/PSS coated electrode sites in three electrode configuration *in vivo*. Working, counter- and reference-electrode were thereby directly integrated in close proximity on the flexible probe, demonstrating that controlled delivery from a three-electrode cell *in vivo* is feasible from a single thin-film based device. During CV stimulations, we could not observe any reaction or sensation in the fully awake animals. This implies that active drug release was performed sub threshold for evoking a neural response. Additionally, we could neither optically nor electrochemically determine any changes to the electrode surfaces nor observe increased inflammation in histology in response to the swept voltage. Similar observations have been made in a recent study by Alba et al. where CV sweeps from -0.9 V to 0.6 V (vs. Pt) were employed for monitoring the CSC for multi-walled carbon nanotube (MWCNT)/Dex modified electrodes in the visual cortex of anesthetized rats [66]. Despite applying more than 200 CV scans during 11 days in their study, they did not observe any changes to the electrode nor any tissue alterations or any influence on the recorded signals in correlation to the CV sweeping. It can thus be concluded that CV cycling is a suitable and, within the herein described boundaries, also safe method to be used for drug release *in vivo* in fully awake animals. This is important considering that CV signals have been reported to be most efficient for driving controlled release of drugs from conducting polymer films [53,59,68].

Furthermore, the previously reported release of by-products in the form of monomers or oligomers [60] could be efficiently controlled by limiting the sweep range in our study, supported by the observation that no additional inflammation was triggered by the release cycles. The limitation of the sweep range thereby did not affect the drug release itself as could be demonstrated in a long-term *in vitro* study over 45 days.

Our Dex-functionalized implants featured an overall drug load of 19 ng per probe, based on the polymerization charge and the doping ratio of PEDOT/Dex. Adopting a tissue volume of $400 \times 400 \times 400$ μm^3 (in relation to the width of the implant) to be treated over 12 weeks, this would allow a Dex concentration of 6.8 μM if the entire drug load is spent over this time. Previous studies have reported on Dex concentrations of 0.2–0.7 μM [53] or 4.5 pg [69] to be efficient for therapeutic cell interaction. This means even if we assume that only a fraction (e.g. 1/10th) of the Dex is released from our PEDOT/Dex coated microprobes over time, the concentration in the tissue would still be high enough demonstrating that electropolymerized PEDOT/Dex coatings with 300 mC cm^{-2} provide sufficient drug storage and release capacity for at least 12 weeks of operation. The maximal drug mass that could theoretically be released from our probes (19 ng) is thereby more than 4 orders of magnitude lower than the neurotoxic levels of Dex reported for hippocampal cells [70].

All PEDOT films were stable over the full 12 weeks which is evident from the monitored impedance data. Stability of the coatings could furthermore be verified by microscopy and SEM imaging of the explanted sample. Based on previously reported results by Boehler et al. [62], such stability is expected for PEDOT/PSS on IrOx but is especially encouraging for PEDOT/Dex which is expected to be more fragile due to the high mobility of the counter ion and the associated mechanical stress in the film during release. The observed stability proves that IrOx is a highly efficient strategy for stabilizing PEDOT films also under *in vivo* conditions and thereby confirms our findings from previous *in vitro* work [62].

By using a flexible substrate material for the probes in our study we were able to keep the entire probe in the tissue during the preparation of histological slices. This technique allowed a precise reconstruction of the actual electrode sites in histology and consequently enabled the direct analysis of tissue in front of the recording/stimulation sites. Examining the number and position of embedded metal tracks, visible in the probe cross-section in histological images, further provided a "bar code" feature which served as simple method for identification of specific electrode sites along the probe shaft.

An unexpected finding is that bare IrOx electrodes outperformed all the PEDOT materials which raises the question whether there are negative effects of PEDOT as such? Considering the large number of studies where PEDOT has been investigated without reporting on negative effects in the literature, this would indeed be a surprising finding. A more likely explanation is the different preconditions in our study where the polyimide probes are exposed to the monomer EDOT during PEDOT deposition, whereas IrOx probes are used as produced in the cleanroom and were never immersed in the monomer solution. We could in fact confirm by HPLC analysis that slight residues from the electrode-position process are present and released from the polyimide surface, bringing them eventually into tissue contact upon probe implantation. Although most of these residues are expected to be cleaned away during immersion of the probes in PBS overnight prior to implantation, further leaching of remaining contaminations over several weeks could be the reason for the slightly elevated inflammation seen around all PEDOT-coated probes in comparison to the IrOx controls. In our study IrOx therefore only has limited suitability as control and tissue reactions should be analysed separately for all PEDOT coated probes. Contaminations from electrolyte residuals could in the future be addressed by improved post-deposition cleaning protocols. The fact that monomer contaminations could be eluted shows that this would indeed be possible by simple immersion in aqueous solutions.

We here show a method for how to use PEDOT/drug systems for local release *in vivo* employing flexible probe technology and three-electrode cell electrochemistry on a single thin-film device with promising qualities. The flexible polyimide devices thereby overall performed exceptionally well regardless of the coating material on

the electrode sites. This is an important outcome since the use of flexible probes has long been limited due to difficulties in precise implantation of such probes. A considerable effort has been invested into developing insertion methods allowing flexible probes to be implanted into brain tissue without buckling or introducing severe tissue damages. We here use a stiff device (optical fibre) as insertion shuttle and confirm that precise implantation of a 10 μm thin flexible probe into the rat hippocampus is possible without significantly harming the surrounding tissue. Although not evaluated or performed in this study, implantation with an optical fibre as guiding tool could in future also be combined with techniques such as optical coherence tomography [71]. By such means, the guidance fibre could provide optical monitoring of the insertion track and thus help to prevent vascular damages or provide improved targeting accuracy within the brain.

Flexible probes generally provide attractive alternatives to stiff implants with respect to tissue reactivity. Nevertheless, stiff implants still provide an important probe technology that cannot readily be replaced by flexible materials in all applications. Controlled release of anti-inflammatory drugs should therefore also be tested with stiff devices where inflammation is expected to be more prominent and thus of higher concerns for long-term applications. We here show that such implementation is technically feasible, however, the effect should still be investigated in combination with stiff probes. Further development of anti-inflammatory electrodes targeting the incorporation of different drugs or investigating the appropriate release timing for optimal treatment efficiency with active drug release technology should be performed. If release is thereby coupled to a surveillance parameter monitoring the extent of inflammation directly at the electrode site, an individual and thus optimal inflammation treatment could be enabled.

5. Conclusion

In conclusion we were able to demonstrate that Dex functionalized PEDOT can be integrated as anti-inflammatory electrode coating on flexible neural microprobes providing unrestricted neural recording properties and low, long-term stable impedance characteristics. Actively controlled release of Dex was possible over 12 weeks using a CV trigger signal in awake animals and data indicates that electrodes exposed to active drug release did have neurons closer to the electrode sites compared to controls, although the effect was not statistically significant. Combining flexible probe technology with anti-inflammatory coatings therefore proves to be a promising approach for enabling long-term stable chronic neural interfaces and should be further developed towards future anti-inflammatory electrode generations.

References

[1] C.-J. Li, Y. Lu, M. Zhou, L.-J. Guo, Electrophysiological properties of hippocampal—cortical neural networks, role in the processes of learning and memory in rats, J. Neural Transm. 121 (2014) 583—592.
[2] M. Weinrich, S.P. Wise, K.H. Mauritz, A neurophysiological study of the premotor cortex in the rhesus monkey, Brain A J. Neurol 107 (1984) 385.
[3] G. Buzsaki, Z. Horvath, R. Urioste, J. Hetke, K. Wise, High-frequency network oscillation in the hippocampus, Science 256 (1992) 1025—1027.
[4] G. Buzsaki, Large-scale recording of neuronal ensembles, Nat. Neurosci. 7 (2004) 446—451.
[5] D.M. Thompson, A.N. Koppes, J.G. Hardy, C.E. Schmidt, Electrical stimuli in the central nervous system microenvironment, Annu. Rev. Biomed. Eng. 16 (2014) 397—430.
[6] P.E. Holtzheimer, H.S. Mayberg, Deep brain stimulation for psychiatric disorders, Annu. Rev. Neurosci. 34 (2011) 289—307.
[7] T. Stieglitz, B. Rubehn, C. Henle, S. Kisban, S. Herwik, P. Ruther, et al., Brain—computer interfaces: an overview of the hardware to record neural signals from the cortex, in: E.M.H.I.H.J.W.A.B.B.G.J.B. Joost Verhaagen, F.S. Dick (Eds.), Progress in Brain Research, Elsevier, 2009, pp. 297—315.
[8] M.L. Homer, A.V. Nurmikko, J.P. Donoghue, L.R. Hochberg, Implants and decoding for intracortical brain computer interfaces, Annu. Rev. Biomed. Eng. 15 (2013) 383—405.
[9] R.A. Normann, E.M. Maynard, P.J. Rousche, D.J. Warren, A neural interface for a cortical vision prosthesis, Vis. Res. 39 (1999) 2577—2587.
[10] W.M. Grill, Signal considerations for chronically implanted electrodes for brain interfacing, in: W.M. Reichert (Ed.), Indwelling Neural Implants: Strategies for Contending with the in Vivo Environment, Taylor & Francis Group, LLC, Boca Raton FL, 2008.
[11] V.S. Polikov, P.A. Tresco, W.M. Reichert, Response of brain tissue to chronically implanted neural electrodes, J. Neurosci. Methods 148 (2005) 1—18.
[12] S. Franz, S. Rammelt, D. Scharnweber, J.C. Simon, Immune responses to implants — a review of the implications for the design of immunomodulatory biomaterials, Biomaterials 32 (2011) 6692—6709.
[13] T.D. Kozai, A.L. Vazquez, C.L. Weaver, S.G. Kim, X.T. Cui, In vivo two-photon microscopy reveals immediate microglial reaction to implantation of microelectrode through extension of processes, J. neural Eng. 9 (2012) 066001.
[14] R. Biran, D.C. Martin, P.A. Tresco, Neuronal cell loss accompanies the brain tissue response to chronically implanted silicon microelectrode arrays, Exp. Neurol. 195 (2005) 115—126.
[15] D.H. Szarowski, M.D. Andersen, S. Retterer, A.J. Spence, M. Isaacson, H.G. Craighead, et al., Brain responses to micro-machined silicon devices, Brain Res. 983 (2003) 23—35.
[16] B.D. Winslow, P.A. Tresco, Quantitative analysis of the tissue response to chronically implanted microwire electrodes in rat cortex, Biomaterials 31 (2010) 1558—1567.
[17] T.D.Y. Kozai, N.B. Langhals, P.R. Patel, X. Deng, H. Zhang, K.L. Smith, et al., Ultrasmall implantable composite microelectrodes with bioactive surfaces for chronic neural interfaces, Nat. Mater. 11 (2012) 1065—1073.
[18] A.B. Schwartz, Cortical neural prosthetics, Annu. Rev. Neurosci. 27 (2004) 487—507.
[19] G.C. McConnell, H.D. Rees, A.I. Levey, C.A. Gutekunst, R.E. Gross, R.V. Bellamkonda, Implanted neural electrodes cause chronic, local inflammation that is correlated with local neurodegeneration, J. neural Eng. 6 (2009) 056003.
[20] R.W. Griffith, D.R. Humphrey, Long-term gliosis around chronically implanted platinum electrodes in the Rhesus macaque motor cortex, Neurosci. Lett. 406 (2006) 81—86.
[21] W.M. Grill, S.E. Norman, R.V. Bellamkonda, Implanted neural interfaces: biochallenges and engineered solutions, Annu. Rev. Biomed. Eng. 11 (2009) 1—24.
[22] M. Welkenhuysen, A. Andrei, L. Ameye, W. Eberle, B. Nuttin, Effect of insertion speed on tissue response and insertion mechanics of a chronically implanted silicon-based neural probe, IEEE Trans. Biomed. Eng. 58 (2011) 3250—3259.
[23] J.P. Seymour, D.R. Kipke, Neural probe design for reduced tissue encapsulation in CNS, Biomaterials 28 (2007) 3594—3607.
[24] T. Stieglitz, H. Beutel, M. Schuettler, J.U. Meyer, Micromachined, polyimidebased devices for flexible neural interfaces, Biomed. Microdevices 2 (2000) 283—294.
[25] P.J. Rousche, D.S. Pellinen, D.P. Pivin, J.C. Williams, R.J. Vetter, D.R. Kipke, Flexible polyimide-based intracortical electrode arrays with bioactive capability, IEEE Trans. Biomed. Eng. 48 (2001) 361—371.
[26] P. Moshayedi, G. Ng, J.C.F. Kwok, G.S.H. Yeo, C.E. Bryant, J.W. Fawcett, et al., The relationship between glial cell mechanosensitivity and foreign body reactions in the central nervous system, Biomaterials 35 (2014) 3919—3925.
[27] K.C. Cheung, P. Renaud, H. Tanila, K. Djupsund, Flexible polyimide microelectrode array for in vivo recordings and current source density analysis, Biosens. Bioelectron. 22 (2007) 1783—1790.
[28] A. Mercanzini, K. Cheung, D.L. Buhl, M. Boers, A. Maillard, P. Colin, et al., Demonstration of cortical recording using novel flexible polymer neural probes, Sensors Actuators A Phys. 143 (2008) 90—96.
[29] T.D. Kozai, A.S. Jaquins-Gerstl, A.L. Vazquez, A.C. Michael, X.T. Cui, Brain tissue responses to neural implants impact signal sensitivity and intervention strategies, ACS Chem. Neurosci. 6 (2015) 48—67.
[30] C. Hassler, J. Guy, M. Nietzschmann, D.T.T. Plachta, J.F. Staiger, T. Stieglitz, Intracortical polyimide electrodes with a bioresorbable coating, Biomed. Microdevices 18 (2016) 81.
[31] A. Richter, Y. Xie, A. Schumacher, S. Loeffler, R. Kirch, J. Al-Hasani, et al., A simple implantation method for flexible, multisite microelectrodes into rat brains, Front. Neuroeng. (2013) 6.
[32] E. Azemi, C.F. Lagenaur, X.T. Cui, The surface immobilization of the neural adhesion molecule L1 on neural probes and its effect on neuronal density and gliosis at the probe/tissue interface, Biomaterials 32 (2011) 681—692.
[33] T. Hickey, D. Kreutzer, D.J. Burgess, F. Moussy, In vivo evaluation of a dexamethasone/PLGA microsphere system designed to suppress the inflammatory tissue response to implantable medical devices, J. Biomed. Mater. Res. 61 (2002) 180—187.

[34] W.K. Ward, J.C. Hansen, R.G. Massoud, J.M. Engle, M.M. Takeno, K.D. Hauch, Controlled release of dexamethasone from subcutaneously-implanted biosensors in pigs: localized anti-inflammatory benefit without systemic effects, J. Biomed. Mater. Res. Part A 94A (2010) 280—287.

[35] S.D. Patil, F. Papadmitrakopoulos, D.J. Burgess, Concurrent delivery of dexamethasone and VEGF for localized inflammation control and angiogenesis, J. Control. Release 117 (2007) 68—79.

[36] M.J. Webber, J.B. Matson, V.K. Tamboli, S.I. Stupp, Controlled release of dexamethasone from peptide nanofiber gels to modulate inflammatory response, Biomaterials 33 (2012) 6823—6832.

[37] W. Shain, L. Spataro, J. Dilgen, K. Haverstick, S. Retterer, M. Isaacson, et al., Controlling cellular reactive responses around neural prosthetic devices using peripheral and local intervention strategies, Neural Syst. Rehabilitation Eng. IEEE Trans. 11 (2003) 186—188.

[38] Y. Zhong, G.C. McConnell, J.D. Ross, S.P. DeWeerth, R.V. Bellamkonda, A novel dexamethasone-releasing, anti-inflammatory coating for neural implants, Neural Engineering, in: Conference Proceedings 2nd International IEEE EMBS Conference on 2005, 2005, pp. 522—525.

[39] Y. Zhong, R.V. Bellamkonda, Dexamethasone-coated neural probes elicit attenuated inflammatory response and neuronal loss compared to uncoated neural probes, Brain Res. 1148 (2007) 15—27.

[40] B.S. Zolnik, D.J. Burgess, Evaluation of in vivo—in vitro release of dexamethasone from PLGA microspheres, J. Control. Release 127 (2008) 137—145.

[41] T.D. Kozai, A.S. Jaquins-Gerstl, A.L. Vazquez, A.C. Michael, X.T. Cui, Dexamethasone retrodialysis attenuates microglial response to implanted probes in vivo, Biomaterials 87 (2016) 157—169.

[42] D.-H. Kim, D.C. Martin, Sustained release of dexamethasone from hydrophilic matrices using PLGA nanoparticles for neural drug delivery, Biomaterials 27 (2006) 3031—3037.

[43] K.A. Potter, M. Jorfi, K.T. Householder, E.J. Foster, C. Weder, J.R. Capadona, Curcumin-releasing mechanically adaptive intracortical implants improve the proximal neuronal density and blood—brain barrier stability, Acta Biomater. 10 (2014) 2209—2222.

[44] U. Bhardwaj, R. Sura, F. Papadimitrakopoulos, D.J. Burgess, Controlling acute inflammation with fast releasing dexamethasone-PLGA microsphere/PVA hydrogel composites for implantable devices, J. diabetes Sci. Technol. 1 (2007) 8—17.

[45] L.W. Norton, H.E. Koschwanez, N.A. Wisniewski, B. Klitzman, W.M. Reichert, Vascular endothelial growth factor and dexamethasone release from nonfouling sensor coatings affect the foreign body response, J. Biomed. Mater. Res. Part A 81A (2007) 858—869.

[46] X. Cui, V.A. Lee, Y. Raphael, J.A. Wiler, J.F. Hetke, D.J. Anderson, et al., Surface modification of neural recording electrodes with conducting polymer/biomolecule blends, J. Biomed. Mater. Res. 56 (2001) 261—272.

[47] X.T. Cui, D.D. Zhou, Poly (3,4-ethylenedioxythiophene) for chronic neural stimulation, IEEE Trans. Neural Syst. Rehabilitation Eng. 15 (2007) 502—508.

[48] A.L. Kip, B.L. Nicholas, D.J. Mike, M.R.-B. Sarah, L.H. Jeffrey, R.K. Daryl, Poly(3,4-ethylenedioxythiophene) (PEDOT) polymer coatings facilitate smaller neural recording electrodes, J. Neural Eng. 8 (2011) 014001.

[49] M. Asplund, T. Nyberg, O. Inganas, Electroactive polymers for neural interfaces, Polym. Chem. 1 (2010) 1374—1391.

[50] D. Svirskis, J. Travas-Sejdic, A. Rodgers, S. Garg, Electrochemically controlled drug delivery based on intrinsically conducting polymers, J. Control. Release Off. J. Control. Release Soc. 146 (2010) 6—15.

[51] V. Pillay, T.-S. Tsai, Y.E. Choonara, L.C. du Toit, P. Kumar, G. Modi, et al., A review of integrating electroactive polymers as responsive systems for specialized drug delivery applications, J. Biomed. Mater. Res. Part A 102 (6) (2014) 2039—2054.

[52] B. Alshammary, F.C. Walsh, P. Herrasti, C. Ponce de Leon, Electrodeposited conductive polymers for controlled drug release: polypyrrole, J. Solid State Electrochem 20 (2016) 839—859.

[53] R. Wadhwa, C.F. Lagenaur, X.T. Cui, Electrochemically controlled release of dexamethasone from conducting polymer polypyrrole coated electrode, J. Control. Release Off. J. Control. Release Soc. 110 (2006) 531—541.

[54] M.R. Abidian, D.H. Kim, D.C. Martin, Conducting-polymer nanotubes for controlled drug release, Adv. Mater. 18 (2006) 405—409.

[55] B. Massoumi, A. Entezami, Electrochemically controlled binding and release of dexamethasone from conducting polymer bilayer films, J. Bioact. Compatible Polym. 17 (2002) 51—62.

[56] G. Stevenson, S.E. Moulton, P.C. Innis, G.G. Wallace, Polyterthiophene as an electrostimulated controlled drug release material of therapeutic levels of dexamethasone, Synth. Met. 160 (2010) 1107—1114.

[57] S. Sirinrath, P. Rajesh, J.W. Thomas, Electrically controlled drug release from nanostructured polypyrrole coated on titanium, Nanotechnology 22 (2011) 085101.

[58] L. Leprince, A. Dogimont, D. Magnin, S. Demoustier-Champagne, Dexamethasone electrically controlled release from polypyrrole-coated nanostructured electrodes, J. Mater Sci. Mater Med. 21 (2010) 925—930.

[59] Y. Xiao, X. Ye, L. He, J. Che, New carbon nanotube—conducting polymer composite electrodes for drug delivery applications, Polym. Int. 61 (2012) 190—196.

[60] C. Boehler, M. Asplund, A detailed insight into drug delivery from PEDOT based on analytical methods: effects and side effects, J. Biomed. Mater. Res. Part A 103 (2015) 1200—1207.

[61] J.S. Ordonez, C. Boehler, M. Schuettler, T. Stieglitz, Improved polyimide thin-film electrodes for neural implants, in: Annual International Conference of the IEEE Engineering in Medicine and Biology Society 2012, 2012, pp. 5134—5137.

[62] C. Boehler, F. Oberueber, S. Schlabach, T. Stieglitz, M. Asplund, Long-term stable adhesion for conducting polymers in biomedical applications: IrOx and nanostructured platinum solve the chronic challenge, ACS Appl. Mater. Interfaces 9 (1) (2017) 189—197.

[63] S.X.Y. Löffler, P. Detemple, A. Moser, U.G. Hofmann, An implantation technique for polyimide based flexible array probes facilitating neuronavigation and chronic implantation, Biomed. Tech. 57 (2012) 860—863.

[64] M.W. Shinwari, D. Zhitomirsky, I.A. Deen, P.R. Selvaganapathy, M.J. Deen, D. Landheer, Microfabricated reference electrodes and their biosensing applications, Sensors 10 (2010) 1679—1715.

[65] H. Yang, S.K. Kang, C.A. Choi, H. Kim, D.-H. Shin, Y.S. Kim, et al., An iridium oxide reference electrode for use in microfabricated biosensors and biochips, Lab a Chip 4 (2004) 42—46.

[66] N. Alba, Z. Du, K. Catt, T. Kozai, X. Cui, In vivo electrochemical analysis of a PEDOT/MWCNT neural electrode coating, Biosensors 5 (2015) 618.

[67] L. Spataro, J. Dilgen, S. Retterer, A.J. Spence, M. Isaacson, J.N. Turner, et al., Dexamethasone treatment reduces astroglia responses to inserted neuroprosthetic devices in rat neocortex, Exp. Neurol. 194 (2005) 289—300.

[68] M. Asplund, C. Boehler, T. Stieglitz, Anti-inflammatory polymer electrodes for glial scar treatment, Front. Neuroeng. 7 (2014) 1—11.

[69] A. Mercanzini, S.T. Reddy, D. Velluto, P. Colin, A. Maillard, J.-C. Bensadoun, et al., Controlled release nanoparticle-embedded coatings reduce the tissue reaction to neuroprostheses, J. Control. Release 145 (2010) 196—202.

[70] L.E. Haynes, M.R. Griffiths, R.E. Hyde, D.J. Barber, I.J. Mitchell, Dexamethasone induces limited apoptosis and extensive sublethal damage to specific subregions of the striatum and hippocampus: implications for mood disorders, Neuroscience 104 (2001) 57—69.

[71] Y. Xie, N. Martini, C. Hassler, R.D. Kirch, T. Stieglitz, A. Seifert, et al., In vivo monitoring of glial scar proliferation on chronically implanted neural electrodes by fiber optical coherence tomography, Front. Neuroeng. 7 (2014) 34.